

# PROCEEDINGS OF SPIE

[SPIDigitalLibrary.org/conference-proceedings-of-spie](https://SPIDigitalLibrary.org/conference-proceedings-of-spie)

## Stabilizing Brillouin lasing in high-Q optical fiber cavity pumped from self-injection locked DFB laser

J. L. Bueno-Escobedo, S. V. Miridonov, Ma. Carmen Maya-Sánchez, D. A. Korobko, I. O. Zolotovskii, et al.

J. L. Bueno-Escobedo, S. V. Miridonov, Ma. Carmen Maya-Sánchez, D. A. Korobko, I. O. Zolotovskii, A. A. Fotiadi, "Stabilizing Brillouin lasing in high-Q optical fiber cavity pumped from self-injection locked DFB laser," Proc. SPIE 12141, Semiconductor Lasers and Laser Dynamics X, 121410J (20 May 2022); doi: 10.1117/12.2621113

**SPIE.**

Event: SPIE Photonics Europe, 2022, Strasbourg, France

# Stabilizing Brillouin Lasing in High-Q Optical Fiber Cavity pumped from self-injection locked DFB laser

J. L. Bueno-Escobedo<sup>a</sup>, S.V. Miridonov<sup>a</sup>, Ma. Carmen Maya-Sánchez<sup>a</sup>,  
D. A. Korobko<sup>b</sup>, I. O. Zolotovskii<sup>b</sup>, A. A. Fotiadi<sup>b,c,d</sup>

<sup>a</sup>Centro de Investigación Científica y de Educación Superior de Ensenada,  
Carretera Ensenada-Tijuana No.3918, Zona Playitas, 22860 Ensenada, B.C., Mexico.

<sup>b</sup>Ulyanovsk State University, 42 Leo Tolstoy Street, Ulyanovsk, 432970, Russia.

<sup>c</sup>Ioffe Physico-Technical Institute of the RAS, 26 Polytekhnicheskaya Street,  
St. Petersburg 194021, Russia.

<sup>d</sup>University of Mons, Boulevard Dolez 31, 7000 Mons, Belgium.

## ABSTRACT

We report on a low-cost Brillouin fiber ring laser pumped from an actively stabilized self-injection locked distributed feedback (DFB) laser diode. Locking of the commercial DFB laser to a ~11-m-length high-Q-factor fiber-optic ring cavity leads to ~10,000-fold narrowing of the laser Lorentzian linewidth down to 400 Hz. Such pump laser operation inside the ring cavity forces the cavity to host Brillouin lasing enabling the laser threshold power as low as ~1.5 mW. The laser operation is perfectly stabilized by active optoelectronic feedback driven by a simple microcontroller. The laser delivers radiation at Stokes frequency with the Lorentzian linewidth reduced down to ~75 Hz and a phase noise less than -100 dBc/Hz (>30 kHz). The reported laser configuration is of great interest for many laser applications where a narrow sub-kHz linewidth, simple design and low cost are important.

**Keywords:** Brillouin distributed sensing; self-injection locking; fiber ring cavity; Brillouin lasers.

## 1. INTRODUCTION

Stimulated Brillouin scattering (SBS) in optical fiber is widely used for many applications, like distributed strain and temperature sensing, selective narrow-bandwidth amplification, optical communication, optical processing of radio-frequency signals, and microwave photonics<sup>1</sup>. Recent progress in the topic is related to high-Q micro-resonators that allow implementing narrow-linewidth frequency-stabilized Brillouin lasers on a silicon chip<sup>2</sup>. An alternative approach is based on fiber-optic resonators that could be simply spliced from standard telecom components. Such flexible and low-cost all-fiber solutions are of particular interest for distributed Brillouin sensing<sup>3-6</sup>, where the fibers with similar Brillouin characteristics could be used. Single-mode Brillouin fiber lasers employing a relatively short fiber-optical ring resonator (FORR) simultaneously resonant to both the pump and Stokes radiations and so referred to as doubly resonant ring cavity lasers, exhibit low threshold, high spectral purity, and low-intensity noise<sup>7-11</sup>. Commonly, such lasers employ a special single-frequency sub-kilohertz pump laser combined with the Pound-Drever-Hall or Hansch-Couillaud active stabilization system<sup>7-13</sup>. However, such technical solutions are rather complicated.

An alternative solution has been proposed recently<sup>14, 15</sup>. We have demonstrated a semiconductor DFB laser operating in self-injection locking regime in a combination with simple active optoelectronic feedback. Such a system enables narrowing of the DFB laser linewidth below ~3 kHz and drastically reduces the laser phase noise<sup>14</sup>. A similar idea can be employed with an all-fiber Brillouin laser, where the fiber-optic ring cavity could be employed simultaneously as an external filtered feedback to narrow the DFB laser linewidth at the pump frequency and as an effective medium to generate Stokes radiation<sup>15</sup>. Potentially, the use of high-Q-factor fiber cavities with such laser configurations could significantly decrease the SBS lasing power threshold, enhance the pump-to-Stokes conversion efficiency and drastically reduce the laser linewidth for a CW Brillouin laser operation. The proper operation of the laser system and its performance characteristics in the configuration with an enhanced FORR Q-factor has not been demonstrated yet.

In this paper, we report on a new single-mode sub-kilohertz Brillouin fiber laser pumped by a self-injection locked pump DFB laser with active stabilization<sup>16</sup>. Specifically, the new laser design comprises a FORR with the Q-factor that is higher than that used with the self-injection locked fiber lasers reported earlier<sup>11-15, 17</sup>. The self-injection locking mechanism provides more than a 10000-fold narrowing of the DFB laser linewidth, whereas the use of the FORR spliced

from only one 99/1 fiber coupler decreases the Stokes threshold down to ~1.5 mW. Active optoelectronic feedback based on a simple microcontroller ensures long-term stabilization of the laser operation at pump and Stokes frequencies, simultaneously. The laser stabilization dynamics, linewidth narrowing, and phase noise reduction in the new fiber laser configuration are experimentally explored.

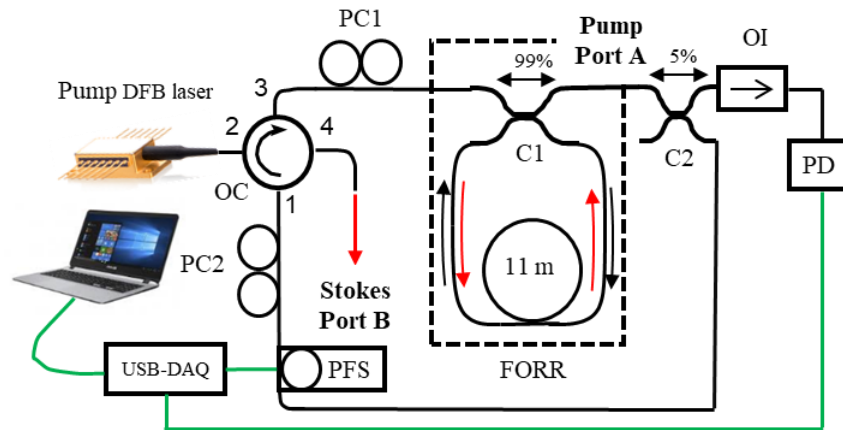


Figure 1. Schematic illustration of the experimental configuration; USB-DAQ - microcontroller, PD –photodetector, OC – 4 ports optical circulator, PC – polarization controller, C – coupler, OI – optical isolator, PFS- piezo fiber stretcher, FORR – fiber-optic ring resonator.

## 2. LASER CONFIGURATION

The experimental laser setup is shown in Fig. 1. A standard distributed feedback (DFB) laser diode supplied by a -30 dB built-in optical isolator generates radiation with a maximal power of ~10 mW at ~1535.5 nm in linear polarization. The laser radiation passes through the optical circulator (OC), polarization controller (PC1), 99/1 coupler (C1), 95/5 coupler (C2), the feedback loop comprising the polarization controller (PC2) and piezo-stretcher (PS), again circulator (OC) and returns back into the DFB laser cavity thus providing passive optical feedback to the laser operation. The 95/5 coupler redirects a part (5%) of the laser power circulating in the feedback loop (port A) that is used for operation of the electronic feedback circuit and spectrum measurements. The FORR optically coupled with the feedback loop is spliced from 99/1 coupler (C1) and contains ~11.33 m of a standard telecom fiber (SMF-28e). The circulator and optical isolators isolate the DFB laser from undesirable back reflections from the fiber faces. The high Q-factor FORR is used simultaneously as a narrow-band optical pass filter attached to the optical feedback loop and as an effective fiber medium to generate Brillouin lasing. Port B of the circulator is used as a Brillouin laser output. The polarization controller (PC1) is used to adjust the polarization state of the light before its introduction to the FORR providing better coupling of the laser radiation with the resonant ring cavity mode. This process could be monitored through the power detected at port A by a fast photodetector (PD, Thorlabs DET08CFC, 5 GHz, 800 - 1700 nm). The polarization controller (PC2) is used to control the optical feedback strength by adjustment of the light polarization state before its injection to the DFB laser emitting a linear polarization. A piezo fiber stretcher (PFS, Evanescent Optics Inc., Model 915B) attached to the feedback loop is used as an optical phase shifter driven by a low-cost USB Multifunction DAQ (National Instrument NI USB-6009) connected with a PC.

## 3. LASER OPERATION AND STABILIZATION

The principle of laser operation in self-injection locking regime is explained in Ref.<sup>18</sup>. The radiation emitted by a DFB laser passes the optical feedback loop and is injected back into the DFB laser cavity forcing the DFB laser to operate the frequency  $\nu_L$  that commonly differs from the frequency  $\nu_{FL}$  generated by a free running DFB laser (the DFB cavity mode frequency). The laser operation frequency  $\nu_L$  is resonant in the coupled laser cavity (comprising the DFB laser cavity and feedback loop), i.e.  $\nu_L = \nu_{FB+LD}$ , where  $\nu_{FB+LD}$  is one of the coupled cavity eigen frequencies. The frequency  $\nu_{FB+LD}$  could be smoothly tuned at least within one free spectrum range (FSR) of the feedback loop by controlling the phase delay in the feedback loop (using a piezo-stretcher, as an example).

Filtered optical feedback is a specific case of optical feedback commonly used with the semiconductor lasers. The use of high-Q external cavities offers the potential to control the DFB laser linewidth through the spectral width of the filter and the detuning from the free running laser frequency  $\nu_{FL}$ <sup>19-21</sup>. For example, in conjugation with a confocal Fabry-Perot resonator the DFB laser could reduce the laser linewidth down to 30 Hz<sup>22</sup>.

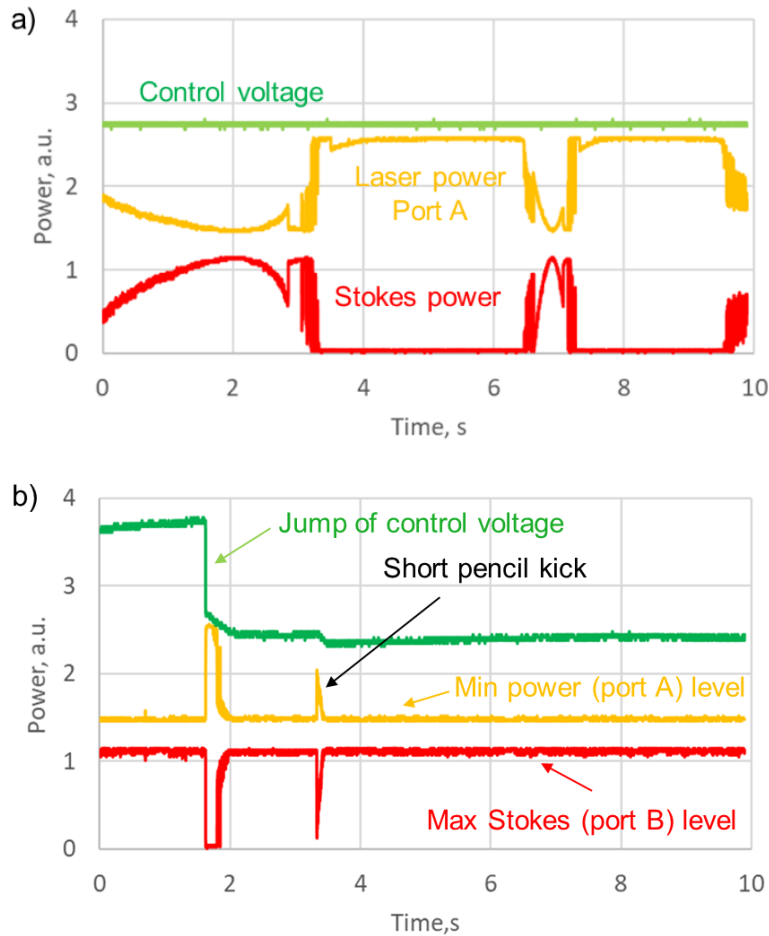


Figure 2. Typical oscilloscopic traces of the reflected and Stokes powers; a) without and b) with active stabilization.

In this context, the laser configuration shown in Fig. 1 could be thought as a DFB laser operating with a simple optical feedback loop coupled with a high Q-factor ring cavity. The isolation provided by the in-built DFB laser isolator is an important parameter of the laser models<sup>21</sup>. To support injection locking it should be between  $-25$  and  $-35$  dB that is a typical isolation of single stage optical fiber isolators. When the laser frequency  $\nu_L$  is out of the ring cavity resonant band, the laser operates like a laser with an optical feedback loop only<sup>19</sup>. The piezo-activator attached to the feedback loop fiber allows to tune  $\nu_L$  affecting the length of the feedback fiber. The effect of high-Q ring cavity brings new features to this process. Using the piezo-activator we can smoothly tune the position of the laser frequency  $\nu_L = \nu_{FB+LD}$  towards the nearest ring cavity resonance mode  $\nu_R$ . Its vicinity to the ring resonance could be monitored through the laser pump power detected at port A. The detected power is maximal when the laser frequency  $\nu_L$  is far from  $\nu_R$  and it is minimal (in our experiment it decreases down to  $\sim 45\%$  of its maximal value) at  $\nu_L = \nu_R$ . With the laser operation frequency  $\nu_L$  approaching the resonance  $\nu_R$ , the laser light circulating inside the fiber feedback loop exhibits strong linewidth narrowing that is the most pronounced at  $\nu_L = \nu_R$ .

The mission addressed to active electronic feedback is to ensure a stable locking of the pump frequency  $\nu_L = \nu_{FB+LD}$  to a ring cavity mode  $\nu_R$  by maintaining the power in port A at its minimal level. A low-cost USB Multifunction DAQ (National Instrument NI USB-6009) connected to a PC is used for this purpose. The laser power detected at port A serves as an error signal. The DAQ output voltage (0 - 5 V) is applied to the piezo-activator controlling the phase delay in the optical fiber loop. The digital control system enables the phase change within the range of  $\pm 20$  rad with a step of  $\pm 0.06$  rad and with a period of  $\sim 3$  ms.

The same fiber ring cavity is used for generation of the Brillouin scattering. Inside the ring, the DFB laser radiation at  $\nu_L$  propagating CW is used as a pump for a Brillouin wave at  $\nu_S = \nu_L - \Delta\nu_{SBS}$  propagating CCW, where  $\Delta\nu_{SBS}$  is the Brillouin frequency shift. To optimize the Brillouin lasing, the ring cavity length  $L_R$  has been precisely adjusted with the single-cut technique<sup>23</sup> to match the Brillouin frequency shift  $\Delta\nu_{SBS}$  and the ring cavity free spectrum range  $FSR \equiv c/nL_R$  as  $\Delta\nu_{SBS} = m_B FSR$ , where  $c$  is the speed of light and  $n$  is the fiber refractive index,  $m_B$  is an integer. With perfectly adjusted fiber ring cavity length, active stabilization of lasing at  $\nu_L = \nu_R$  ensures stabilization of lasing at the frequency  $\nu_S$ .

#### 4. EXPERIMENTAL RESULTS

With the laser configuration shown in Fig. 1 lasing at the pump frequency  $\nu_L$  and at the Stokes frequency  $\nu_S$  has been monitored through ports A and B, respectively. The signal from port A is detected by a fast photodetector and is used as an error signal for the active feedback operation.

Figure 2 compares oscilloscope traces recorded for the control signal applied to the piezo-stretcher, pump and Brillouin powers without and with active feedback. For the laser operating without electronic feedback the laser frequency  $\nu_L = \nu_{FB+LD}$  is not locked to the ring resonance  $\nu_R$ . Driven by an environment noise both frequencies  $\nu_L$  and  $\nu_R$  slowly (and almost independently) vary in time forcing the power detected in port A to walk between its minimal and maximal values. Most of the time the laser frequency  $\nu_L$  does not match the ring cavity resonant band and, therefore, the laser radiation passes through the fiber ring coupler with a loss of less than  $\sim 1\%$  of its power. When the frequencies  $\nu_L$  and  $\nu_R$  occasionally approach each other, the laser power detected at port A decreases and the CW pump power circulating inside the ring drastically increases. Once getting the Brillouin lasing threshold, this power generates the CCW Stokes wave in the ring emitted through port B at  $\nu_S$ . Energy conversion from the pump to Stokes wave maintains the laser power detected at port A at the level corresponding to the Brillouin threshold. When the pump power inside the ring falls below the Brillouin threshold, lasing at the Stokes frequency drops out.

The laser operation with supplementary electronic feedback is shown in Fig. 2(b). The electronic feedback circuit is trying to maintain the laser pump power detected at port A (now it is used as an error signal) fixed to its minimal value. So, the DFB laser frequency  $\nu_L$  is always locked to the ring cavity mode  $\nu_R$  providing a stable laser operation at the pump and Brillouin frequencies recorded at ports A and B, respectively ( $\nu_L = \nu_R = \nu_{FB+LD}$ ). One can see that the self-injection locking mechanism in combination with optoelectronic feedback perfectly works against the environment noise enabling stable laser operation at two locked frequencies. Sometimes, the stabilized laser behavior could be interrupted by a short mode-hopping event provoked by the environment noise. Fig. 2(b) shows the system response to a pencil kick on the fiber configuration. One can see, both optical signals (and so the pump laser frequency  $\nu_L$ ) deviate from the steady-state point and then quickly returns to the original position. A typical time of the restoration governed by active electronic feedback is  $\tau_L \sim 0.2$  s for both pump and Stokes signals.

Another source of the laser instabilities is a drift of environment temperature. Commonly, the fiber configuration is placed into a foam box, but no additional thermal control of the box is applied. The environmental temperature variations affect both the ring cavity and feedback loop fiber lengths changing the mutual position of the resonant frequencies  $\nu_R$  and  $\nu_L$ . The electronic feedback circuit works against the temperature noise trying to maintain the equality  $\nu_L = \nu_R$ . To this end, it controls the phase delay in the optical feedback loop smoothly changing the voltage applied to the piezo-stretcher. The dynamical range of the piezo-stretcher is limited by  $\pm 20$  rad. When this limit is exhausted, the phase must be reset by an integer number of circles. Such jumps of the control signal destabilize the laser

for a short time (like, it is shown in Fig.2(b)). A typical time of the stabilized laser operation in the laboratory environment (between two jumps of the control signal) is ~5-7 min.

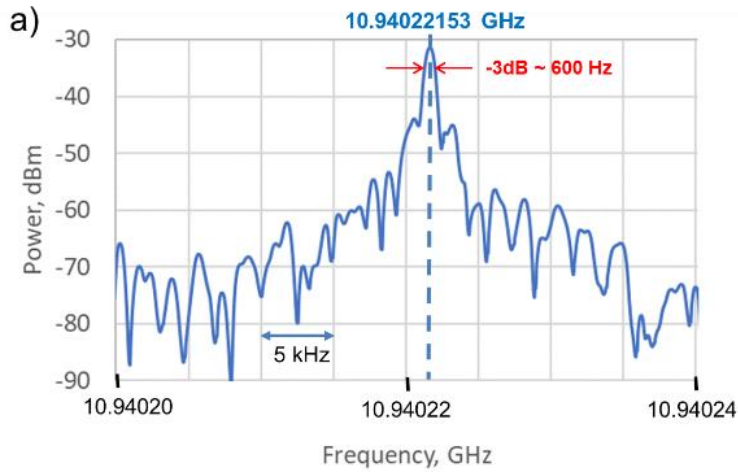


Figure 3. RF beat spectrum acquired for ~20ms

Figure 3 shows a typical radiofrequency (RF) spectrum recorded by an RF signal analyzer (Keysight N9040B, 50GHz) with an acquisition time of ~20 ms and characterizing beating between pump and Stokes laser outputs. One can see that the typical RF spectrum exhibits a pronounced peak centered at ~10.9402 GHz and with the width of ~600 Hz. The recorded peak frequency corresponds to the Brillouin frequency shift in the ring cavity fiber (SMF-28, Corning Inc.) at 1535 nm and room temperature.

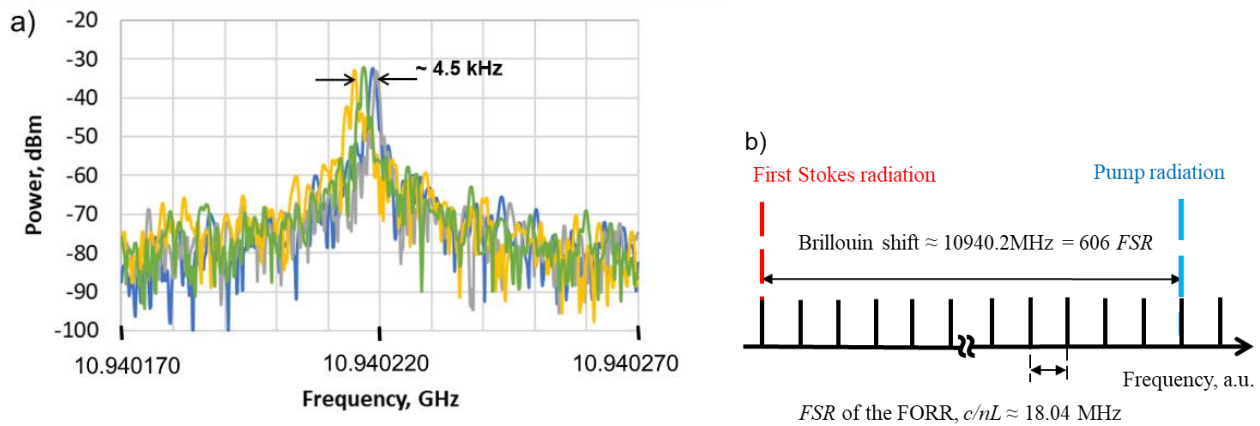


Figure 4. a) RF beat spectrum realizations taken during 1 h with the thermally stabilized laser setup. b) Mode structure in the Brillouin laser cavity with double resonance.

To stabilize the laser permanently we have used thermal control applied to the laser box as a whole, thus enabling mode-hopping free laser operation. The RF spectrum measurements similar to that shown in Fig.3 have been repeated several times during 1 h [Fig.4 (a)]. Exclusively, for this experiment, the laser box has been put in a chamber stabilized at ~23°C. No mode hopping has been detected for this time. The variation of the RF spectrum peak position  $\delta\nu_{RF} < 4.5$  kHz reflects the effect of the residual temperature fluctuations. Using these data one can estimate the value of the Brillouin laser frequency drift  $\delta\nu_s$  caused by the temperature noise. Indeed, both the pump and Stokes laser frequencies are locked to the ring cavity modes as shown in Fig. 4(b) and so their difference measured as the RF spectrum peak position  $\nu_{RF}$  should be an integer number of the ring cavity free spectrum ranges (FSR):

$$\nu_{RF} = \nu_p - \nu_s = (p - s)FSR \quad (1)$$

where  $p$  and  $s$  are orders of the ring cavity modes associated with pump and Stokes lasing.

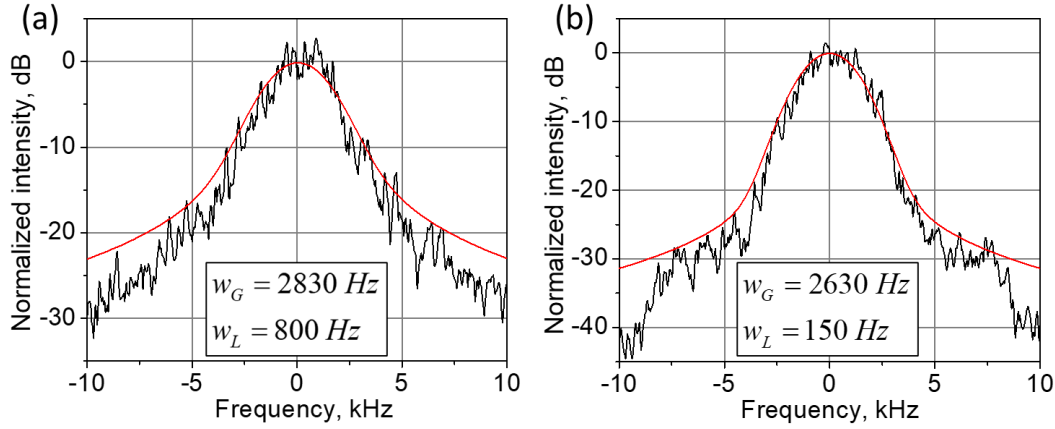


Figure 5. Delayed self-heterodyne spectra of the laser radiation emitted through ports A (a) and B (b) at pump and Stokes laser frequencies, respectively. The measured spectra (black) and their fitting Voigt profiles (red) with the Gaussian and Lorentzian linewidths (FWHM)  $w_G$  and  $w_L$ , respectively, as the fitting parameters.

Therefore, the link between the variations of the Brillouin laser frequency  $\nu_s$  and the RF spectrum peak position  $\nu_s$  could be expressed as:

$$\delta\nu_s = \frac{s}{(p - s)} \delta\nu_{RF} \quad (2)$$

With the pump mode orders estimated as  $s = 1.08 \cdot 10^7$  and  $p - s = 606$ , the deviation of the Brillouin laser frequency for 1 h is limited by  $\delta\nu_s < 80 \text{ MHz}$ . So, we can conclude that that when the laser frequency is trapped within the boundaries of  $\pm 40 \text{ MHz}$ , the laser operation remains to be stabilized permanently. Using the same technique, we have estimated the drift of the Brillouin laser frequency in the laser without an external thermal control. In this case, a drift of the RF spectrum peak frequency with an average velocity of  $\sim 450 \text{ Hz/min}$  corresponding to the drift of the Brillouin laser frequency  $\sim 8 \text{ MHz/min}$  has been measured. Such environment conditions enable a stable laser operation for  $\sim 5\text{-}7$  min before the control signal jump destabilizes the laser, since the Brillouin laser frequency drift exhausts the limit of the piezo-stretcher dynamical range.

The RF beat spectrum characteristics are in a good quantitative agreement with the Stokes and pump optical linewidths measured with the delayed self-heterodyne technique<sup>24-27</sup>. An all-fiber unbalanced Mach-Zehnder interferometer with a 55 km delay fiber supplied by 20 MHz phase modulator has been used for this purpose. The beat signal from the interferometer is detected by a  $\sim 5 \text{ GHz}$  photodiode and analyzed by an RF spectrum analyzer (FSH8, Rohde & Schwarz). The experimental spectra shown in Fig. 5 are averaged over 10 independent measurements each lasting for  $\sim 92.2$  ms. Both spectra are centered around  $20 \text{ MHz}$ . The narrower spectrum (recorded with the Stokes output) exhibits oscillations in the wings evidencing that the laser coherence length is much longer than the interferometer delay fiber<sup>25</sup>. To proceed the measured data, we use the method based on the decomposition of the self-heterodyne spectra into Gaussian and Lorentzian contributions<sup>26, 27</sup>. In this approach, the laser's line is thought to be Gaussian in the range near the top, and Lorentzian in the wings. The Lorentzian and Gaussian contributions can be evaluated by fitting the measured self-heterodyne spectrum by the Voigt profile. Figure 5 shows the fitting Voigt profiles obtained using the algorithm described in<sup>27</sup>. One can see that the fitting is applied just to the highest points in the wings ensuring upper values of the Lorentzian laser linewidths estimated for two laser outputs. The Lorentzian laser linewidth is a half of the Lorentzian width (FWHM)  $w_L$  of self-heterodyne spectrum and the Gaussian component is  $\sqrt{2}/2$  times the Gaussian linewidth (FWHM)  $w_G$  of self-heterodyne spectrum<sup>26</sup>. Therefore, the natural Lorentzian laser linewidths are found to be narrower than 400 Hz and 75 Hz for the pump and Stokes laser outputs, respectively. For comparison, the optical spectrum linewidth of the free running DFB laser diode is  $\sim 4 \text{ MHz}$ .

Figure 6 shows the first Stokes power as a function of the pump power at the FORR input. One can see that the emitted Stokes power increases with an increase of the input pump power linearly up to  $\sim 5.5$  mW that is believed to be the threshold power of the second Stokes generation. Above the threshold the first Stokes power does not change more with the increase of the input pump power due to its conversion to the second Stokes radiation generated in the ring cavity co-directly to the pump. The insert in Fig.6 demonstrates the second peak of the pump radiation optical spectra shifted by  $\sim 0.16$  nm (equivalent to  $-2\Delta\nu_{SBS}$ ) from the main peak highlighting the presence of the second Stokes radiation emitted through the pump radiation output.

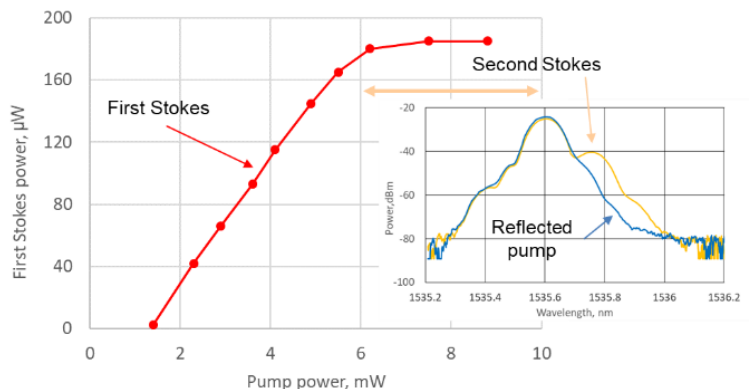


Figure 6. The Stokes power as a function of the pump power and optical spectra recorded at port A (inset).

Figure 7 shows the noise performance of the Brillouin laser. The power spectral density (PSD) of phase noise recorded for the pump and Stokes radiations with a RF spectrum analyzer (Agilent N9320A) in the range of 10–100 kHz is presented in Fig.7 (a). For the used RF spectrum range, the effect of active feedback noise on the laser performance is negligible. The PSDs have been measured by the self-heterodyne method<sup>28-30</sup> using an unbalanced Mach-Zehnder interferometer with a  $\sim 1.3$  km delay fiber ( $\sim 5.76$   $\mu$ s) and 20 MHz frequency shifter. One can see that beyond 30 kHz the active stabilization circuit keeps the phase noise of the pump radiation below  $-80$  dBc/Hz. Comparing the pump laser output (port A) the PSD measured with Brillouin laser output (port B) is lower by  $\sim (10-25)$  dBc/Hz over the range. We believe that it is the result of filtering effect in the high-Q-factor ring cavity.

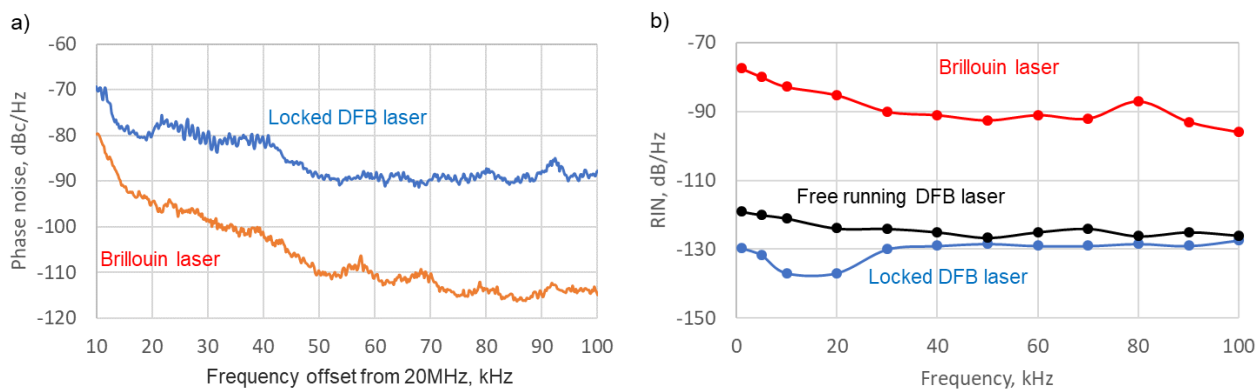


Figure 7. Noise performance of the laser locked at  $\nu_L = \nu_R$  : a) Phase noise; b) Relative Intensity noise (RIN). Relative intensity noise of free running pump laser (black points) is shown for comparison.

Figure 7(b) presents the relative intensity noise (RIN) measured with a lock-in amplifier SRS510 in 1–100 kHz frequency range. One can see that the RIN of stabilized pump laser is lower by  $\sim (5-10)$  dB than the RIN of free-running DFB laser. At the same time, the RIN of the Stokes radiation (port B) is higher by 30–40 dB than the RIN of the pump laser output (port A), especially at lower frequencies. We explain this increase by an exponential manner of the Stokes wave amplification in the fiber ring cavity resulting in a strong pump-to-Stokes RIN transfer.



## 4. DISCUSSION

We have introduced a simple Brillouin laser based on a DFB laser coupled to an all-fiber ring cavity and working in self-injection-locking regime. In our laser configuration, the same high-Q-factor ring fiber cavity is exploited both for self-injection locking of the DFB laser and for generation of Stokes light via stimulated Brillouin scattering. A low-cost USB-DAQ is used to stabilize the system preventing mode-hopping. Importantly, the self-injection locking mechanism maintains permanent coupling between the DFB laser and the external fiber ring cavity enabling perfect resonant pumping for low-noise Brillouin lasing.

In contrast to the previous laser configurations<sup>11-15</sup>, we have employed the fiber ring cavity built (and then incorporated into the configuration) using just one fiber coupler instead of two couplers used earlier. Such cavity design potentially reduces the optical losses in the ring cavity (twice in comparison with Ref.<sup>15</sup>) providing an enhanced Q-factor. Thanks to new Brillouin laser design, the laser performance characteristics has been significantly improved. The Brillouin laser output is increased up to  $\sim 180 \mu W$  from  $\sim 100 \mu W$  reported with the two-coupler ring configuration<sup>15</sup>. Further power scaling is still possible with an external amplifier (it could be a Brillouin amplifier built from the same fiber). The Brillouin lasing threshold power is reduced down to  $\sim 1.5 \text{ mW}$  comparing with  $\sim 2.9 \text{ mW}$  observed with longer ring cavity ( $\sim 20 \text{ m}$ )<sup>15</sup>. The Brillouin laser Lorentzian linewidth is reduced down to  $\sim 75 \text{ Hz}$  from  $\sim 110 \text{ Hz}$  measured earlier in the same way. To the best of our knowledge, it is the narrowest laser linewidth reported with the self-injection locked DFB lasers employing an external fiber cavity<sup>11-15, 17, 18</sup>.

Qualitatively, the laser performance characteristics shown in Fig.2-6 are not so different from the similar characteristics reported with the previous laser configurations<sup>14, 15</sup>. There is a crucial difference, however. Indeed, in most of the laser configurations, the feedback signal is maximized when the laser gets locked to a cavity mode. In our case, it takes its minimum value (see Fig.2(b)), raising the question, whether the same mechanism governs the laser locking here. Although the detailed theoretical description of the laser operation is under progress (and out of scope of this paper), we believe, there are no contradiction between the mentioned feature and current understanding<sup>20</sup>. Indeed, it is commonly accepted that for lasers operating in the injection locking regime mode hopping not necessarily occurs from the mode with higher to the mode with lower losses. In contrast, at sufficiently high feedback level (and laser phase noise), when multiple solutions exist for the phase condition, the laser frequency locks to the mode with the lowest phase noise level (mode hopping occurs from the mode with wider laser linewidth to the mode with lower laser linewidth). Thus, the laser locks more and more to the feedback phase adjusted for minimum linewidth until further mode hopping is suppressed. Apparently, the laser behavior in our experiment follows this scenario. When the phase delay tuned by the piezo-stretcher pushes the laser frequency  $\nu_L$  to the ring cavity resonance  $\nu_R$ , a decrease of the feedback signal (in two times only) is accompanied by a drastic narrowing of the laser linewidth (more than an order of magnitude) thus providing an increasingly strong locking of the laser to the ring cavity resonance  $\nu_R$ .

When the injection locking regime is established, the laser frequency  $\nu_L$  is locked to the frequency  $\nu_R$  ( $\nu_L = \nu_R$ ) and to the frequency  $\nu_{FB+LD}$ , simultaneously. Under other conditions being equal (the laser diode current and temperature are well stabilized, the lasing power does not change), the environmental temperature variations affect the ring cavity and feedback loop fiber lengths changing the mutual position of the resonant frequencies  $\nu_R$  and  $\nu_{FB+LD}$ . A deviation of  $\nu_R$  from  $\nu_{FB+LD}$  (or versa) disrupts the injection locking destabilizing the laser. To avoid this, the position of  $\nu_{FB+LD}$  should be permanently adjusted to  $\nu_R$ . It is the task of the active feedback circuit to maintain the equality  $\nu_{FB+LD} = \nu_R$ . In Ref.<sup>14</sup> the active feedback has been implemented through the control of laser diode current. However, this solution is limited by rather a small range of the allowed current modulation. Along with the desirable frequency  $\nu_{FB+LD}$  control, the laser current modulation could disturb the DFB laser parameters (power, temperature, gain) producing poorly predictable effects on the system behavior. In contrast, the phase control through a piezo-stretcher may directly tune  $\nu_{FB+LD}$  just affecting the length of the feedback loop fiber. It makes this control mechanism more practical, exhibiting much better stability and reproducibility. However, a limited dynamical range of the piezo-stretcher possesses restraints on the laser operation as well. When the limit is exhausted the phase must be reset and a jump of the control signal destabilizes the system. The use of an additional thermal control applied to the whole laser configuration allows to handle the laser frequency drifts making the laser operation permanently stabile.

## 5. CONCLUSION

In conclusion, we have experimentally demonstrated a single-mode sub-kilohertz Brillouin fiber ring laser just splicing a commercial DFB laser and a few standard telecom components. The laser delivers a CW narrowband radiation at pump and Stokes frequencies, simultaneously. The DFB laser diode is optically locked to the resonance frequency of the 11.33-m length fiber optic ring resonator providing  $\sim 10\,000$  times Lorentzian linewidth narrowing down to  $\sim 400$  Hz. The pump laser operation is perfectly stabilized by active optoelectronic feedback driven by a simple microcontroller. Accumulation of the pump laser radiation inside the ring cavity forces the ring cavity to operate as the CW Brillouin laser delivering the Stokes light with Lorentzian linewidth of  $\sim 75$  Hz above the pump power threshold of  $\sim 1.5$  mW. The relative intensity noise of the Stokes radiation is  $< -90$  dB/Hz, and the phase noise is  $< -100$  dBc/Hz for RF frequencies  $> 30$  kHz. Such characteristics are of interest for many laser applications, including high-resolution spectroscopy, phase coherent optical communications, distributed fiber optics sensing<sup>31-34</sup>, coherent optical spectrum analyzer, and microwave photonics<sup>35-40</sup>. Further research will be directed to design and testing of new fiber laser sources and devices with unique performance characteristics dedicated for these applications<sup>41-53</sup>.

## ACKNOWLEDGEMENTS

The work was supported by the Ministry of Higher Education and Science of the Russian Federation (Megagrant Program, project #075-15-2021-581) and the Russian Science Foundation (project 18-12-00457P). The construction of the thermal stabilization system was supported by the Russian Fund of Basic Research (19-42-730009 p\_a).

## REFERENCES

- [1] Agrawal, G., [Nonlinear fiber optics], © Academic Press 2001 (2001).
- [2] Loh, W., Green, A. A. S., Baynes, F. N., Cole, D. C., Quinlan, F. J., Lee, H., Vahala, K. J., Papp, S. B., and Diddams, S. A., "Dual-microcavity narrow-linewidth brillouin laser," *Optica* **2**, 225-232 (2015).
- [3] Soto, M. A., [Distributed brillouin sensing: Time-domain techniques], Springer, Singapore (2018).
- [4] Bao, X., and Chen, L., "Recent progress in brillouin scattering based fiber sensors," *Sensors* **11**, 4152-4187 (2011).
- [5] Gorshkov, B. G., Yüksel, K., Fotiadi, A. A., Wuilpart, M., Korobko, D. A., Zhirnov, A. A., Stepanov, K. V., Turov, A. T., Konstantinov, Y. A., and Lobach, I. A., "Scientific applications of distributed acoustic sensing: State-of-the-art review and perspective," *Sensors* **22**, 1033 (2022).
- [6] Lopez-Mercado, C. A., Korobko, D. A., Zolotovskii, I. O., and Fotiadi, A. A., "Application of dual-frequency self-injection locked dfb laser for brillouin optical time domain analysis," *Sensors (Basel)* **21** (2021).
- [7] Norcia, S., Tonda-Goldstein, S., Dolfi, D., Huignard, J. P., and Frey, R., "Efficient single-mode brillouin fiber laser for low-noise optical carrier reduction of microwave signals," *Optics Letters* **28**, 1888-1890 (2003).
- [8] Geng, J., Staines, S., Wang, Z., Zong, J., Blake, M., and Jiang, S., "Highly stable low-noise brillouin fiber laser with ultranarrow spectral linewidth," *IEEE Photonics Technology Letters* **18**, 1813-1815 (2006).
- [9] Molin, S., Baili, G., Alouini, M., Dolfi, D., and Huignard, J.-P., "Experimental investigation of relative intensity noise in brillouin fiber ring lasers for microwave photonics applications," *Optics Letters* **33**, 1681-1683 (2008).
- [10] Korobko, D. A., Zolotovskii, I. O., Svetukhin, V. V., Zhukov, A. V., Fomin, A. N., Borisova, C. V., and Fotiadi, A. A., "Detuning effects in brillouin ring microresonator laser," *Opt Express* **28**, 4962-4972 (2020).
- [11] Spirin, V. V., López-Mercado, C. A., Mégret, P., and Fotiadi, A. A., "Single-mode brillouin fiber laser passively stabilized at resonance frequency with self-injection locked pump laser," *Laser Physics Letters* **9**, 377-380 (2012).
- [12] Bueno Escobedo, J. L., Spirin, V. V., López-Mercado, C. A., Mégret, P., Zolotovskii, I. O., and Fotiadi, A. A., "Self-injection locking of the dfb laser through an external ring fiber cavity: Polarization behavior," *Results in Physics* **6**, 59-60 (2016).
- [13] Spirin, V. V., López-Mercado, C. A., Kinet, D., Mégret, P., Zolotovskiy, I. O., and Fotiadi, A. A., "A single-longitudinal-mode brillouin fiber laser passively stabilized at the pump resonance frequency with a dynamic population inversion grating," *Laser Physics Letters* **10**, 015102 (2013).
- [14] Spirin, V. V., Bueno Escobedo, J. L., Korobko, D. A., Mégret, P., and Fotiadi, A. A., "Stabilizing dfb laser injection-locked to an external fiber-optic ring resonator," *Opt. Express* **28**, 478-484 (2020).

- [15] Spirin, V. V., Bueno Escobedo, J. L., Korobko, D. A., Mégret, P., and Fotiadi, A. A., "Dual-frequency laser comprising a single fiber ring cavity for self-injection locking of dfb laser diode and brillouin lasing," *Opt. Express* **28**, 37322-37333 (2020).
- [16] Spirin, V. V., Bueno Escobedo, J. L., Miridonov, S. V., Maya Sánchez, M. C., López-Mercado, C. A., Korobko, D. A., Zolotovskii, I. O., and Fotiadi, A. A., "Sub-kilohertz brillouin fiber laser with stabilized self-injection locked dfb pump laser," *Optics & Laser Technology* **141**, 107156 (2021).
- [17] Wei, F., Yang, F., Zhang, X., Xu, D., Ding, M., Zhang, L., Chen, D., Cai, H., Fang, Z., and Xijia, G., "Subkilohertz linewidth reduction of a dfb diode laser using self-injection locking with a fiber bragg grating fabry-perot cavity," *Opt. Express* **24**, 17406-17415 (2016).
- [18] López-Mercado, C. A., Spirin, V. V., Bueno Escobedo, J. L., Márquez Lucero, A., Mégret, P., Zolotovskii, I. O., and Fotiadi, A. A., "Locking of the dfb laser through fiber optic resonator on different coupling regimes," *Optics Communications* **359**, 195-199 (2016).
- [19] Petermann, K., [Laser diode modulation and noise], Springer Science & Business Media (2012).
- [20] Ohtsubo, J., [Semiconductor lasers: Stability, instability and chaos], Springer (2012).
- [21] Korobko, D. A., Zolotovskii, I. O., Panajotov, K., Spirin, V. V., and Fotiadi, A. A., "Self-injection-locking linewidth narrowing in a semiconductor laser coupled to an external fiber-optic ring resonator," *Optics Communications* **405**, 253-258 (2017).
- [22] Laurent, P., Clairon, A., and Breant, C., "Frequency noise analysis of optically self-locked diode lasers," *IEEE Journal of Quantum Electronics* **25**, 1131-1142 (1989).
- [23] Spirin, V. V., López-Mercado, C. A., Kablukov, S. I., Zlobina, E. A., Zolotovskiy, I. O., Mégret, P., and Fotiadi, A. A., "Single cut technique for adjustment of doubly resonant brillouin laser cavities," *Optics Letters* **38**, 2528-2531 (2013).
- [24] Derickson, D., Hentschel, C., and Vobis, J., [Fiber optic test and measurement], Prentice Hall PTR New Jersey (1998).
- [25] Richter, L. E., Mandelberg, H. I., Kruger, M. S., and Mcgrath, P. A., "Linewidth determination from self-heterodyne measurements with subcoherence delay times," *Ieee Journal of Quantum Electronics* **22**, 2070-2074 (1986).
- [26] Mercer, L. B., "1 / f frequency noise effects on self-heterodyne linewidth measurements," *IEEE Lightwave Technology* **9**, 485-493 (1991).
- [27] Chen, M., Meng, Z., Wang, J., and Chen, W., "Ultra-narrow linewidth measurement based on voigt profile fitting," *Opt. Express* **23**, 6803-6808 (2015).
- [28] Camatel, S., and Ferrero, V., "Narrow linewidth cw laser phase noise characterization methods for coherent transmission system applications," *Journal of Lightwave Technology* **26**, 3048-3055 (2008).
- [29] Llopis, O., Merrer, P. H., Brahim, H., Saleh, K., and Lacroix, P., "Phase noise measurement of a narrow linewidth cw laser using delay line approaches," *Optics Letters* **36**, 2713-2715 (2011).
- [30] Li, Y., Fu, Z., Zhu, L., Fang, J., Zhu, H., Zhong, J., Xu, P., Chen, X., Wang, J., and Zhan, M., "Laser frequency noise measurement using an envelope-ratio method based on a delayed self-heterodyne interferometer," *Optics Communications* **435**, 244-250 (2019).
- [31] Bueno Escobedo, J. L., Jason, J., López-Mercado, C. A., Spirin, V. V., Wuilpart, M., Mégret, P., Korobko, D. A., Zolotovskiy, I. O., and Fotiadi, A. A., "Distributed measurements of vibration frequency using phase-otdr with a dfb laser self-stabilized through pm fiber ring cavity," *Results in Physics* **12**, 1840-1842 (2019).
- [32] Bueno Escobedo, J. L., Spirin, V. V., López-Mercado, C. A., Márquez Lucero, A., Mégret, P., Zolotovskii, I. O., and Fotiadi, A. A., "Self-injection locking of the dfb laser through an external ring fiber cavity: Application for phase sensitive otdr acoustic sensor," *Results in Physics* **7**, 641-643 (2017).
- [33] Fotiadi, A. A., Brambilla, G., Ernst, T., Slattery, S. A., and Nikogosyan, D. N., "Tpa-induced long-period gratings in a photonic crystal fiber: Inscription and temperature sensing properties," *Journal of the Optical Society of America B: Optical Physics* **24**, 1475-1481 (2007).
- [34] Faustov, A. V., Gusarov, A. V., Mégret, P., Wuilpart, M., Zhukov, A. V., Novikov, S. G., Svetukhin, V. V., and Fotiadi, A. A., "The use of optical frequency-domain reflectometry in remote distributed measurements of the  $\gamma$ -radiation dose," *Technical Physics Letters* **41**, 414-417 (2015).
- [35] Marpaung, D., Morrison, B., Pagani, M., Pant, R., Choi, D.-Y., Luther-Davies, B., Madden, S. J., and Eggleton, B. J., "Low-power, chip-based stimulated brillouin scattering microwave photonic filter with ultrahigh selectivity," *Optica* **2**, 76-83 (2015).
- [36] Balram, K. C., Davanço, M. I., Song, J. D., and Srinivasan, K., "Coherent coupling between radiofrequency, optical and acoustic waves in piezo-optomechanical circuits," *Nature Photonics* **10**, 346 (2016).

- [37] Li, J., Suh, M.-G., and Vahala, K., "Microresonator brillouin gyroscope," *Optica* **4**, 346-348 (2017).
- [38] Suh, M. G., Lai, Y. H., and Vahala, K. J., "Microresonator brillouin laser gyroscope with earth-rotation-rate sensitivity," in *2021 Optical Fiber Communications Conference and Exhibition (OFC)*(2021), pp. 1-3.
- [39] Morrison, B., Casas-Bedoya, A., Ren, G., Vu, K., Liu, Y., Zarifi, A., Nguyen, T. G., Choi, D.-Y., Marpaung, D., Madden, S. J., Mitchell, A., and Eggleton, B. J., "Compact brillouin devices through hybrid integration on silicon," *Optica* **4**, 847-854 (2017).
- [40] Merklein, M., Stiller, B., and Eggleton, B. J., "Brillouin-based light storage and delay techniques," *Journal of Optics* **20**, 083003 (2018).
- [41] Phan Huy, K., Nguyen, A. T., Brainis, E., Haelterman, M., Emplit, P., Corbari, C., Canagasabey, A., Kazansky, P. G., Deparis, O., Fotiadi, A. A., Mégret, P., and Massar, S., "Photon pair source based on parametric fluorescence in periodically poled twin-hole silica fiber," *Opt. Express* **15**, 4419 (2007).
- [42] Ribenek, V. A., Stoliarov, D. A., Korobko, D. A., and Fotiadi, A. A., "Pulse repetition rate tuning of a harmonically mode-locked ring fiber laser using resonant optical injection," *Optics Letters* **46**, 5687-5690 (2021).
- [43] Ribenek, V. A., Stoliarov, D. A., Korobko, D. A., and Fotiadi, A. A., "Mitigation of the supermode noise in a harmonically mode-locked ring fiber laser using optical injection," *Optics Letters* **46**, 5747-5750 (2021).
- [44] Khashi, H. J., Sergeev, S. V., Al-Araimi, M., Rozhin, A., Korobko, D., and Fotiadi, A., "High-frequency vector harmonic mode locking driven by acoustic resonances," *Optics Letters* **44**, 5112-5115 (2019).
- [45] Lobach, I. A., Drobyshev, R. V., Fotiadi, A. A., Podivilov, E. V., Kablukov, S. I., and Babin, S. A., "Open-cavity fiber laser with distributed feedback based on externally or self-induced dynamic gratings," *Optics Letters* **42**, 4207 (2017).
- [46] Korobko, D. A., Fotiadi, A. A., and Zolotovskii, I. O., "Mode-locking evolution in ring fiber lasers with tunable repetition rate," *Opt. Express* **25**, 21180 (2017).
- [47] Lobach, I. A., Kablukov, S. I., Podivilov, E. V., Fotiadi, A. A., and Babin, S. A., "Fourier synthesis with single-mode pulses from a multimode laser," *Optics Letters* **40**, 3671 (2015).
- [48] Fotiadi, A. A., Korobko, D. A., Zolotovskii, I. O., and Taylor, J. R., "Brillouin-like amplification in rare-earth-doped optical fibers," *Opt. Express* **29**, 40345-40359 (2021).
- [49] Preda, C. E., Fotiadi, A. A., and Megret, P., "Numerical approximation for brillouin fiber ring resonator," *Opt Express* **20**, 5783-5788 (2012).
- [50] Brambilla, G., Fotiadi, A. A., Slattery, S. A., and Nikogosyan, D. N., "Two-photon photochemical long-period grating fabrication in pure-fused-silica photonic crystal fiber," *Optics Letters* **31**, 2675 (2006).
- [51] Caucheteur, C., Fotiadi, A., Megret, P., Slattery, S. A., and Nikogosyan, D. N., "Polarization properties of long-period gratings prepared by high-intensity femtosecond 352-nm pulses," *IEEE Photonics Technology Letters* **17**, 2346-2348 (2005).
- [52] Gruk, D. A., Kurkov, A. S., Razdobreev, I. M., and Fotiadi, A. A., "Self-q-switched ytterbium-doped cladding-pumped fibre laser," *Quantum electronics* **32**, 1017 (2002).
- [53] Popov, S. M., Butov, O. V., Bazakutsa, A. P., Vyatkin, M. Y., Chamorovskii, Y. K., and Fotiadi, A. A., "Random lasing in a short er-doped artificial rayleigh fiber," *Results in Physics* **16**, 102868 (2020).